Inorg. Chem. **2006**, *45*, 1243–1251

Structural and Texture Evolution with Temperature of Layered Double Hydroxides Intercalated with Paramolybdate Anions

D. Carriazo,[†] C. Domingo,[‡] C. Martín,[†] and V. Rives*[,†]

Departamento de Química Inorgánica, Universidad de Salamanca, 37008-Salamanca, Spain, and Instituto de Estructura de la Materia, CSIC, Serrano 123, 28006-Madrid, Spain

Received May 30, 2005

Paramolybdate-LDHs with MgAl or ZnAl cations within the layers have been prepared by the ion-exchange method from hydrotalcites with different interlayer anions (OH^-, NO_3^-, and terephthalate). The samples and the oxides obtained after their calcination were characterized by element chemical analysis, PXRD, FT-Raman spectroscopy, thermal analysis (TG/DTA), N_2 adsorption at –196 °C, and SEM. The results show that layered solids with hydrotalcite-type structure were obtained in which the interlayer space is occupied by heptamolybdate with a small amount of MoO_4^{2-} units formed through hydrolysis of the polyanion; both oxomolybdenum species undergo a progressive distortion of the octahedral units from 50 °C but are roughly stable up to 250 °C as a consequence of the interaction between the polyanion and the brucite-like layers. This distortion is responsible for the observed decrease in the height of the gallery for samples heated in the temperature range, 50–250 °C, with respect to the original samples. Rehydration of the calcined solids allows recovering of their original structures and the initial values for the gallery heights. Calcination between 300 and 400 °C gives rise to a collapse of the layered structure, and amorphous phases are formed, in which molybdenum is both octahedrally and tetrahedrally coordinated. Crystalline magnesium and zinc molybdates ($MgMoO_4$ and $ZnMoO_4$) are formed at 450 and 600 °C, respectively. All solids have some microporosity, which decreases with increasing the calcination temperature.

Introduction

Layered double hydroxides (LDHs), also known as anionic clays or hydrotalcite-type (HT) compounds, form a group of minerals with the general formula $[M^{2+}_{1-x}M^{3+}_x(OH)_2]A_{x/n}^{n-}\cdot mH_2O$. The M^{2+} and M^{3+} cations are located in $[M(OH)_6]$ edge-sharing octahedra with the brucite structure, and anions (A^{n-}) are located, together with water molecules, in the interlayer region.[1−4] Many metal cations are able to form this sort of compound, and consequently, a very large number of compounds with this structure have been synthesized in recent years, varying the nature and molar ratio of cations in the interlayer and the nature of the interlayer anions.[1−4] Polyxometalates (POMs) display a large structural diversity and are largely used in medicine, materials science, and catalysis.[5−7] Their strong Brönsted type acidity[8] and their redox properties make them attractive in different catalytic reactions. However, they are hardly recyclable and their specific surface area is usually rather low, so giving rise to a low density of active sites. One way to overcome this problem is to immobilize them on different solid supports, such as LDHs, forming hybrid materials.[9−12]

Pinnavaia et al.[13] intercalated decavanadate and Keggin ions ($XM_{12}O_{40}^{n-}$) using the nitrate form of a Zn,Al hydrotalcite as a precursor. Afterward, several authors reported preparation of LDH−POMs systems by reconstruction of the

* To whom correspondence should be addressed. E-mail: vrives@usal.es.
† Universidad de Salamanca.
‡ Instituto de Estructura de la Materia.

(1) Reichle, W. T. *Solid State Ionics* **1986**, *22*, 135.
(2) Cavani, F.; Trifiró, F.; Vaccari, A. *Catal. Today* **1991**, *11*, 1.
(3) Rives, V.; Ulibarri, M. A. *Coord. Chem. Rev.* **1999**, *181*, 61.
(4) *Layered Double Hydroxides: Present and Future*; Rives, V., Ed.; Nova Sci. Pub., Inc.: New York, 2001.
(5) Katsoulis, D. E. *Chem. Rev.* **1998**, *98*, 359.
(6) Mizuno, N.; Misono, M. *Chem. Rev.* **1998**, *98*, 199.
(7) Kozhevnikov, I. V. *Chem. Rev.* **1998**, *98*, 171.
(8) Furuta, M.; Sakata, K.; Misono, M.; Yoneda, Y. *Chem. Lett.* **1979**, 31.
(9) Misono, M. *Catal. Rev.*—Sci. Eng. **1987**, *29*, 269.
(10) Rozheunikov, I. V.; Sinnema, A.; Jansen, R. J. J.; Pamin, K.; van Bekkum, H. *Catal. Lett.* **1995**, *30*, 241.
(11) Kresge, C. T.; Marler, D. O.; Rav., G. S.; Rose, B. H. U.S. Patent 5,366,945, 1994.
(12) Schwegler, M. A.; van Bekkum, H.; de Munck, N. A. *Appl. Catal.* **1991**, *74*, 191.
(13) Kwon, K.; Tsigdinos, G. A.; Pinnavaia, T. J. *J. Am. Chem. Soc.* **1988**, *110*, 3653.

10.1021/ic0508674 CCC: $33.50
Published on Web 12/27/2005

layered structure from partially calcined LDHs or by anion exchange, using LDHs with both organic or inorganic intercalated anions.[2,3,14−20]

The structure of the POMs is usually pH-dependent,[21] and they tend to depolymerize in the basic medium provided by the LDH suspension; therefore, the experimental conditions during synthesis (i.e., pH, temperature, contact time between the solid and the solution, etc.) should be carefully controlled. In addition, the precise nature of the POM (responsible for balancing the positive charge of the layers) is also important through the charge/size ratio in the POM: POMs with a low charge/size ratio cannot be intercalated in LDHs with high positive layer charge.

Although many reports have been published on the intercalation of Keggin and other heteropolyoxometalates, only a few number of papers have dealt with intercalation of heptamolybdate.[22−25] In all cases, a layered phase with a basal spacing close to 12 Å ($2\theta = 7.3°$) is formed. However, no definitive agreement exists on the evolution of the interlayer phase with temperature: In some cases, a fast reaction between heptamolybdate and layer cations has been claimed;[23] in some other cases it seems that heptamolybdate anion keeps its structure up to 400 °C,[22] and depolymerization or even grafting have been also claimed.[26−29]

We here report the intercalation by anion exchange of heptamolybdate in LDHs containing Mg,Al or Zn,Al in the layers; the different nature of the layer cations gives rise to different acid−base properties, and exchange has been made starting with LDHs containing hydroxide, nitrate, or terephthalate as interlayer anion, to analyze their effect on the exchange process and the nature and stability of the final LDH−POM material.

The layered LDH−POM compounds, as well as the compounds obtained upon thermal decomposition at increasing temperatures (from 80 to 900 °C), have been characterized by different physicochemical techniques. We aimed to analyze the effect of the LDH precursors on the structure and porosity of the LDH−POM hybrid compound, as well as to identify the evolution of the Mo-containing species during calcination, to gain information on the nature of the calcined species. The thermal study for these materials is important because not only LDH−POMs, but also the mixed oxides obtained after their calcination, are suitable heterogeneous catalysts for oxidation processes.

Experimental Section

Samples Preparation. All chemicals were from Fluka (Buchs, Switzerland) and were used without any further purification.

Five precursor LDHs were prepared. The Mg,Al−OH (meixnerite) hydrotalcite was prepared from a Mg,Al−CO_3 sample (hereafter MgAlC) with a molar Mg/Al ratio of two, which had been previously prepared by following the method described by Reichle.[30] A portion (3 g) of sample MgAlC was calcined in N_2 at 500 °C for 3 h, and the resulting solid was suspended in 200 mL of water. The suspension was kept for 2 days at 70 °C and maintained under nitrogen atmosphere until used for exchange.

The Zn,Al−NO_3 and Mg,Al−NO_3 (hereafter ZnAlN and MgAlN, respectively) hydrotalcites were prepared by coprecipitation following the method previously described by Gardner and Pinnavaia[23] and Arco et al.,[31] respectively. The precipitates were centrifuged and washed with water several times; a portion was dried in a vacuum and was used for full characterization, while the remaining suspension was kept under N_2 atmosphere for further exchange with heptamolybdate.

The Mg,Al and Zn,Al hydrotalcites containing interlayer terephthalate (here after MgAlT and ZnAlT, respectively) were prepared following methods similar to those previously described by Drezdzon[14] and Crespo et al.,[32] respectively. In both cases, the precipitates were treated as above-described for samples MgAlN and ZnAlN.

In all cases the starting solutions were prepared with a M^{2+}/Al^{3+} molar ratio of 2.0 and decarbonated water was used for preparing the solutions and for washing the precipitates.

All the heptamolybdate-containing LDHs were prepared by anion exchange under an inert atmosphere as follows: 50 mL of an aqueous solution of ammonium heptamolybdate (hereafter AHM) was added to 100 mL of the precursor suspension (the solid precursor was not isolated prior to exchange because it is well-known that in such a case deaggregation of the primary particles is difficult and thus exchange as well). The amount of AHM was 50% larger than the anion exchange capacity of the starting LDHs (in other words, 50% larger than that required for balancing the positive charge due to the presence of Al^{3+} cations in the brucite-like layers). Once the addition had been completed, a few drops of 2 M HNO_3 were added until a constant pH value of 4.5 was reached, and then the suspension was stirred at 30 °C for 1 h (samples containing terephthalate), 24 h at 30 °C (ex-meixnerite sample), or 24 h at 60 °C (samples containing nitrate); the solid was then centrifuged, washed, and dried in a vacuum in a desiccator. The samples will be named as XYMo, where X = Mg or Zn and Y = Mx,N,T for those prepared from precursor LDHs containing hydroxide, nitrate, or terephthalate, respectively, in the interlayer. Contact time between the suspensions and the solids, as well as reaction temperature, were chosen after systematic study of optimum experimental conditions.

Characterization Procedures. All samples prepared, as well as the solids obtained after thermal decomposition up to 900 °C, have been characterized using different experimental techniques.

(14) Drezdzon, M. A. *Inorg. Chem.* **1988**, *27*, 4628.
(15) Nijs, H.; de Bock, M.; Vansant, E. F. *J. Porous Mater.* **1999**, *6*, 101.
(16) Kwon, T.; Pinnavaia, T. J. *Chem. Mater.* **1989**, *1*, 381.
(17) Kwon, T.; Pinnavaia, T. J. *J. Mol. Catal.* **1992**, *74*, 23.
(18) Kooli, F.; Jones, W. *Inorg. Chem.* **1995**, *34*, 6237.
(19) Dimotakis, E. D.; Pinnavaia, T. J. *Inorg. Chem.* **1990**, *29*, 2393.
(20) Ulibarri, M. A.; Labajos, F. M.; Rives, V.; Trujillano, R.; Kagunya, W.; Jones, W. *Inorg. Chem.* **1994**, *33*, 2592.
(21) Pope, M. T. *Heteropoly and Isopoly Oxometalates*; Springer-Verlag: New York, 1983.
(22) Twu, J.; Dutta, P. K. *Chem. Mater.* **1992**, *4*, 398.
(23) Gardner, E.; Pinnavaia, T. J. *Appl. Catal., A* **1998**, *167*, 65.
(24) Mitchell, P. C. H.; Wass, S. A. *Appl. Catal., A* **2002**, *225*, 153.
(25) Tatsumi, T.; Yamamoto, K.; Tajina, H.; Tominaga, H. *Chem. Lett.* **1992**, 895.
(26) Wang, J.; Tian, Y.; Wang, R. C.; Clearfield, A. *Chem. Mater.* **1992**, *4*, 1276.
(27) Narita, E.; Kaviratna, P. D.; Pinnavaia, T. J. *J. Chem. Soc., Chem. Commun.* **1993**, 60.
(28) Weber, R. S.; Gallezot, P.; Lefebre, F.; Suib, S. L. *Microporous Mater.* **1993**, *1*, 223.
(29) del Arco, M.; Carriazo, D.; Gutiérrez, S.; Martín, C.; Rives, V. *Inorg. Chem.* **2004**, *43*, 375.
(30) Reichle, W. T. *J. Catal.* **1985**, *94*, 547.
(31) del Arco, M.; Gutiérrez, S.; Martín, C.; Rives, V.; Rocha, J. *J. Solid State Chem.* **2000**, *151*, 272.
(32) Crespo, I.; Barriga, C.; Rives, V.; Ulibarri, M. A. *Solid State Ionics* **1997**, *101*, 729.

Table 1. Chemical Composition (% Weight) and Formulas of the Samples Prepared

sample	% M^{2+}	% Al	% C	% N	% Mo	M^{2+}/Al^{3+} [a]	formula
MgAlC	16.41	10.45	2.31			1.7	$[Mg_{0.63}Al_{0.36}(OH)_2](CO_3)_{0.18}{\cdot}nH_2O$
MgAlN	18.47	10.10		5.24		2.0	$[Mg_{0.67}Al_{0.33}(OH)_2](NO_3)_{0.33}{\cdot}nH_2O$
MgAlT	17.65	10.88	19.24			1.8	$[Mg_{0.64}Al_{0.36}(OH)_2](TA)_{0.18}{\cdot}nH_2O$
MgMxMo	9.46	6.78			29.23	1.6	$[Mg_{0.61}Al_{0.39}(OH)_2](Mo_7O_{24})_{0.065}{\cdot}nH_2O$
MgNMo	9.16	6.74			26.09	1.5	$[Mg_{0.60}Al_{0.40}(OH)_2](Mo_7O_{24})_{0.07}{\cdot}nH_2O$
MgTMo	9.56	7.03			26.09	1.5	$[Mg_{0.60}Al_{0.40}(OH)_2](Mo_7O_{24})_{0.065}{\cdot}nH_2O$
ZnAlN	31.20	6.43		3.2		2.0	$[Zn_{0.67}Al_{0.33}(OH)_2](NO_3)_{0.32}{\cdot}nH_2O$
ZnAlT	30.80	7.83	13.26			1.6	$[Zn_{0.62}Al_{0.38}(OH)_2](TA)_{0.19}{\cdot}nH_2O$
ZnNMo	25.23	5.20			24.93	2.0	$[Zn_{0.66}Al_{0.33}(OH)_2](Mo_7O_{24})_{0.06}{\cdot}nH_2O$
ZnTMo	24.09	5.25			24.09	1.9	$[Zn_{0.66}Al_{0.34}(OH)_2](Mo_7O_{24})_{0.06}{\cdot}nH_2O$

[a] Experimental molar ratio.

Element chemical analyses were carried out at the Servicio General de Análisis Químico Aplicado (University of Salamanca, Salamanca, Spain); Mg, Al, Zn, and Mo were determined by atomic absorption in a Mark-2 EEL 240 apparatus, after dissolving the samples in nitric acid, while carbon content was determined in a CHNS 932 Leco analyzer.

The powder X-ray diffraction (PXRD) patterns were obtained by reflection from powder packed in a sample holder, with a Siemens D-500 diffractometer, using Cu Kα radiation ($\lambda = 1.540\,50$ Å) with a graphite monochromator and interfaced to a DACO-MP data acquisition microprocessor. The diagrams were recorded in the 5−70° (2θ) range at a scan speed of 0.05° s^{-1} and a time constant of 1.5 s. The crystalline phases were identified from comparison with database software (JCPDS files).[33]

Differential thermal analyses (DTA) and thermogravimetric (TG) analyses were recorded in DTA-7 and TG-7 instruments, respectively, from Perkin-Elmer. The analyses were carried out in flowing (30 mL min^{-1}) nitrogen from L'Air Liquide (Valladolid, Spain) at a heating rate of 10 °C min^{-1}.

FT-Raman spectra were recorded in a Bruker RFS-100 instrument, using the 1064 nm line of a Nd:YAG laser as excitation source. Dispersive Raman spectra at 785 and 514 nm laser wavelengths were obtained with a confocal Raman microscope from Reinshaw, RM-2000, equipped with a Leica microscope, and an electrically refrigerated CCD camera. The spectra were taken with 50× and 20× objectives (0.75 and 0.40 NA, respectively) with laser powers ranging from 10 to 30 mW; integration times were in the 300−500 s range.

The nitrogen adsorption−desorption isotherms for specific surface area and porosity assessment were recorded at −196 °C in a Gemini instrument from Micromeritics; specific surface areas were determined by the Brunauer−Emmett−Teller (BET) method.[34]

Scanning electron micrographs were obtained in a model 940 digital scanning microscope from Zeiss.

Results and Discussion

Element Chemical Analyses. Results for all samples prepared are summarized in Table 1. The M^{2+}/Al^{3+} molar ratio is close, but in many cases lower, than the value in the starting solution (2.0) for the precursor samples. The value for the Mo-containing samples is, however, rather small (1.6−1.5) for the samples containing Mg^{2+}, but 1.9−2.0 for those prepared with Zn^{2+}. Such a deviation from the expected value of 2.0 has been reported previously,[4] and it has been ascribed to a preferential dissolution of the divalent cation during exchange, probably because of the low pH of the solution during the preparation; the larger basicity of the Mg,Al than the Zn,Al series favors dissolution of Mg^{2+} in a larger extent than Zn^{2+}.

It is well-known that the nature of the oxomolybdenum species depends on the pH, tetrahedral at pH > 10 but octahedral at pH < 6, and the nuclearity of the POM increases as the pH is decreased.[21] The predominating species at pH used for exchange (4.5) is $Mo_7O_{24}^{6-}$, and this species has been assumed to exist in these solids, thus giving rise to the formulas included in Table 1. The $Al^{3+}/Mo_7O_{24}^{6-}$ ratio is close to 6, thus further evidencing the presence of this oxomolybdenum species in the interlayer.

The metal contents in the samples calcined at 80−200 °C is larger than in the original samples due to removal of water (see TG results below), but the molar ratio between metal contents is maintained.

Despite for sample ZnAlN a small amount of ZnO seems to exist (see the PXRD section below), the formula has been calculated by assuming all Zn^{2+} cations are in the brucite-like layers; the amount of ZnO seems to be rather small, and the molar Al^{3+}/NO_3^- ratio would be unchanged whether the presence of ZnO is taken into account or not; in any case, the formula given should be obviously taken as an approximate one.

Powder X-ray Diffraction. The diagrams for the precursors are included in Figure 1A and are characteristic of the hydrotalcite-like structure. The first diffraction peak has been ascribed to planes (003), assuming a *R*3*m* symmetry stacking of the brucite-like layers; it is recorded at 8.8 (sample MgAlN), 8.9 (ZnAlN), and 14.1 Å (MgAlT and ZnAlT), corresponding to 2θ values of 10.0, 9.9, and 6.2°, respectively. The first two values are in agreement[23,31] with the interlayer nitrate anions located with their C_3 axis parallel to the layers. The terephthalate anions are located upward in both ZnAlT and MgAlT samples.[14,32,35,36] In addition, very weak diffraction lines at 10.6 ($2\theta = 8.2°$) and 5.3 Å ($2\theta = 16.7°$) are recorded for sample MgAlT, Figure 1A, which can be tentatively ascribed to the presence of a minor second phase where the terephthalate anions adopt a different orientation in the interlayer, as the value is too high to

(33) Joint Committee on Powder Diffraction Standards, International Centre for Diffraction Data, Swarthmore, PA, 1977.
(34) Brunauer, S.; Emmett, P. H.; Teller, E. *J. Am. Chem. Soc.* **1938**, *60*, 309.
(35) Vucelic, M.; Moggridge, G. D.; Jones, W. *J. Phys. Chem.* **1995**, *99*, 8328.
(36) Roy, A.; Forano, C.; Besse, J. P. In *Layered Double Hydroxides: Present and Future*; Rives, V., Ed.; Nova Sci. Pub., Inc.: New York, 2001; Chapter 1, p 1.

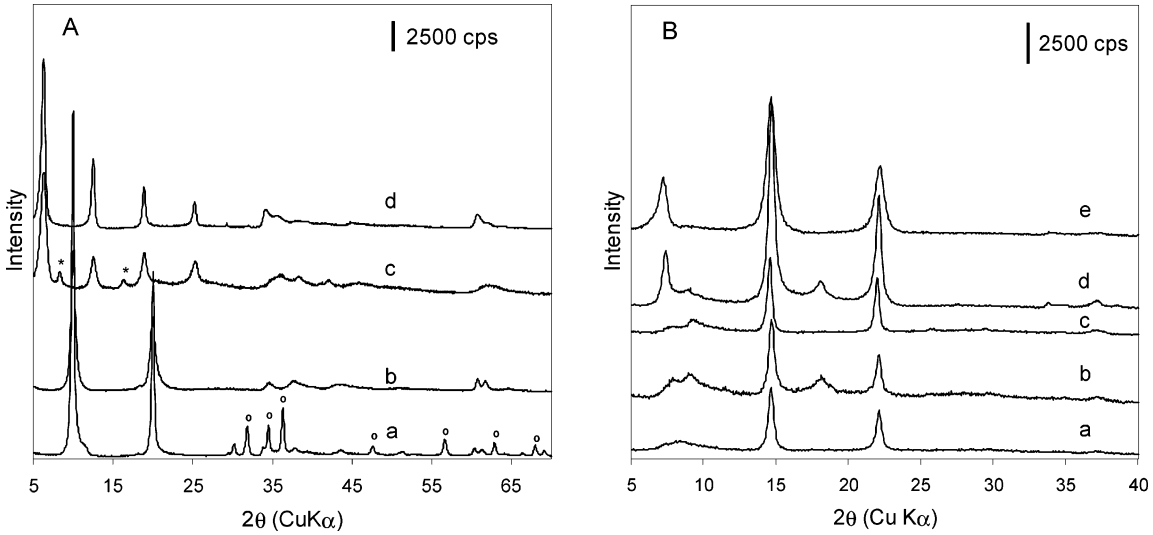

Figure 1. (A) PXRD patterns of the precursor samples (a) ZnAlN, (b) MgAlN, (c) MgAlT, and (d) ZnAlT. (B) XRD patterns of oriented films of (a) MgTMo, (b) MgNMo, (c) MgMxMo, (d) ZnNMo, and (e) ZnTMo. Key: (∗) terephthalate oriented parallel to brucite-like layers; (*o*) ZnO (zincite).

correspond to a Mg,Al−NO_3 hydrotalcite. The PXRD diagram for sample ZnAlN shows also some weak diffraction maxima due to zincite, ZnO (JCPDS file 36-1451), a species rather usually found coprecipitated with Zn-containing hydrotalcites.[37]

Anion exchange introducing heptamolybdate anions, whatever the hydrotalcite precursor used, gives rise to solids also showing a hydrotalcite-like structure; the corresponding PXRD diagrams, recorded using the oriented aggregated method, are shown in Figure 1B. Basal reflections are recorded at 12, 6, and 4 Å (2θ = 7.3, 14.7, and 22.2°, respectively). The first diffraction peak is usually the strongest one in the PXRD diagrams of these solids; however, in this case it is less intense than the second peak and even in some cases it is recorded as a shoulder to a more intense diffraction maximum. These opposite intensities for the (00*l*) maxima has been previously reported by several authors for different LDHs containing polyoxometalates in the interlayer space,[13−29,38] and it has been ascribed to the presence of atoms with large atomic scattering factors in the interlayer.[38] In the diagrams recorded for unoriented powder samples, the first diffraction peak is more intense and is recorded as a rather broad band between 12 and 9.8 Å (2θ = 7.3−9.0°), probably due to the presence of a second crystalline phase, responsible for the peak between 11 and 9.8 Å (2θ = 8.05−9.0°).

The $d_{(003)}$ value of 12 Å (2θ = 7.3°) was previously reported by some authors[22−25] and, after subtracting the thickness of the brucite-like layers (4.8 Å[14]), coincides with the height calculated, by using Crystal Maker software,[39] for the $[Mo_7O_{24}]^{6-}$ anion with its C_2 axis perpendicular to the brucite-like layers; in this orientation, maximum interaction between the polyoxometalate and the hydroxyl groups of the layers is achieved.

The diagrams recorded for samples MgNMo and ZnNMo show a diffraction at 4.9 Å (2θ = 18°) in addition to the basal diffractions at 12, 6, and 4 Å (2θ = 7.3, 14.7, and 22.2°, respectively) and the broader diffraction maximum at 11−9.8 Å (2θ = 8.05−9.0°). Its intensity increases with the synthesis temperature, and its absence in the diagrams of the ex-terephthalate and ex-meixnerite samples is due to the lower temperature used to prepare this series of samples.

We also observed that the diffraction lines at 11−9.8 Å (2θ = 8.05−9.0°) and 4.9 Å (2θ = 18°) are recorded and even become stronger, when any of the solids prepared was calcined at increasing temperatures, and these are the only signals recorded when the sample is calcined between 80 and 200 °C, Figure 2.

No clear diffraction maximum is recorded when the calcination temperature is increased to 300 °C, Figure 2, thus showing that the layered structure has collapsed, leading to amorphous solids. The amorphous phase is detected even when the samples are calcined at 600 (sample MgAl−POM) or 450 °C (sample ZnAl−POM), and above these temperatures new diffraction lines, which intensity increase as the calcinations temperature is further increased, are again recorded. So, for sample MgAl−POM calcined at 600 °C (and even clearer when the calcinations is performed at 700−800 °C), the diffraction lines at 4.67, 3.37, and 3.28 Å (2θ = 19.0, 26.4, and 27.1°, respectively) are characteristic of monoclinic $MgMoO_4$ (JPCDS file 21-0961), where Mo ions are octahedrally coordinated by oxide anions. However, diffraction lines due to $MgMo_2O_7$ or $MgAl_2O_4$, which have been reported by other authors,[22] are not recorded, and then we should conclude that in the Mg-containing samples aluminum-containing species should be amorphous or very well dispersed. Calcination of sample ZnAl−Mo_7O_{24} at 450 °C leads to formation of $ZnMoO_4$ (JCPDS file 35-0765). A further increase in the calcinations temperature gives rise to development of diffraction maxima at 3.6, 2.69, and 2.6 Å (2θ = 24.7, 33.2, and 34.4°, respectively), probably due to $Zn_3Mo_2O_9$ (JCPDS file 21-1483), and diffraction lines due

(37) Kooli, F.; Depege, C.; Ennaqadi, A.; de Roy, A.; Besse, J. P. *Clay Clay Miner.* **1997**, *45*, 92.
(38) Hibino, T.; Tsunashima, A. *Chem. Mater.* **1997**, *9*, 2082.
(39) Crystal Maker, version 2.1.0.: http//www.crystalmaker.co.uk/cristal-maker.

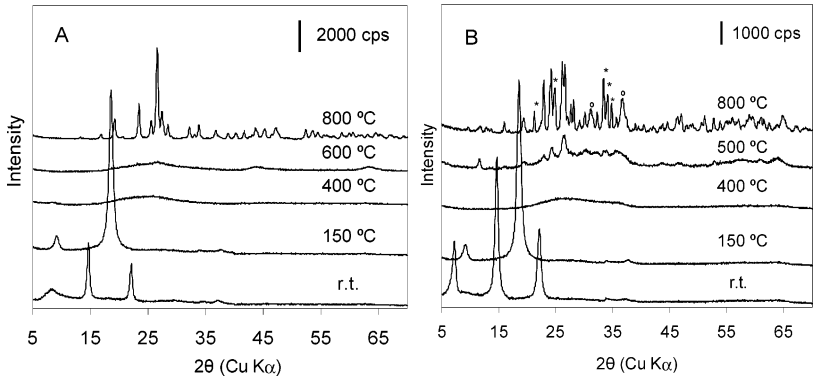

Figure 2. PXRD patterns of (A) MgTMo and (B) ZnTMo calcined at different temperatures. Key: (∗) $Zn_3Mo_2O_9$; (*o*) $ZnAl_2O_4$.

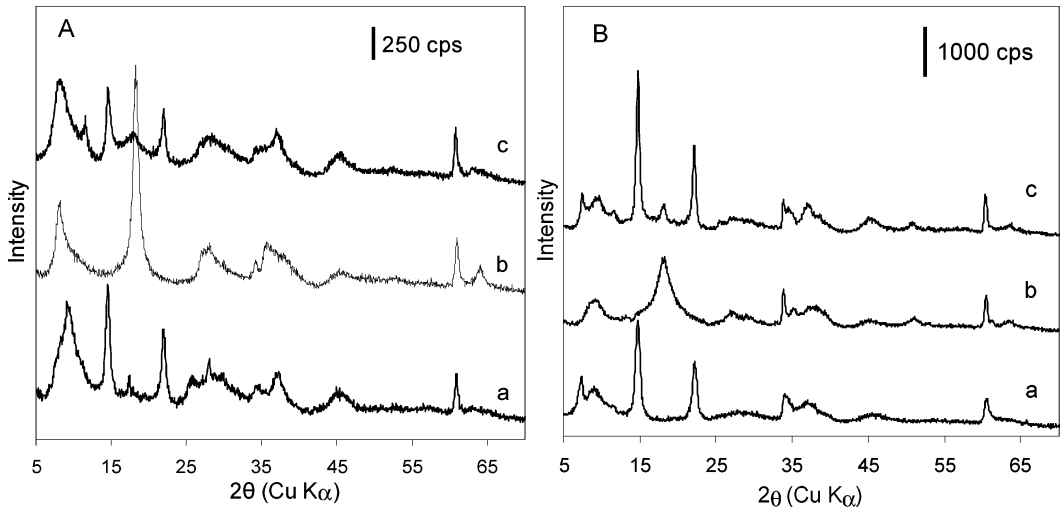

Figure 3. (A) PXRD patterns of MgNMo samples (a) uncalcined, (b) calcined at 120 °C, and (c) after hydration of sample b. (B) PXRD patterns of ZnTMo samples (a) uncalcined, (b) calcined at 90 °C, and (c) after hydration treatment of sample b.

to normal spinel $ZnAl_2O_4$ (JCPDS file 5-0669) are recorded when the sample is calcined at 800 °C.

The origin of the diffraction lines close to 11−9.8 Å (2θ = 8.05−9.0°) and 4.9 Å (2θ = 18°) is not clear. Some authors have claimed that the first line, recorded in the PXRD diagram of several POM-containing hydrotalcites, is due to ill-crystallized Mg and/or Al polyoxometalates.[23] This should be the only remaining crystalline phase after heating at 80 °C. However, other authors have pointed out that this line is due to polyoxometalate grafting to the brucite-like layers, upon displacement of some hydroxyl groups from the layers by oxide anions of the POM moiety.[26,29] Partial depolymerization of the polyoxmetalate,[26−28] or a mixture of POM together with small anions in the interlayer,[38] has been also claimed as being the origin of this diffraction line.

For insight into the origin of these lines, we have mixed an aqueous solution containing Al^{3+} and Mg^{2+} (or Zn^{2+}) cations with an aqueous solution of ammonium heptamolybdate; the mixture was heated at 80 °C and pH = 4.5 (HNO_3), to reproduce as close as possible the experimental conditions during anion exchange. No precipitate was observed in any case; the diffraction diagram of the solid residue formed upon evaporation of the solvent does not show any diffraction line close to 11−9.8 Å (2θ = 8.05−9.0°) and 4.9 Å (2θ = 18°). These diffraction lines are not recorded after mixing either MgAl−CO_3 or ZnAl−CO_3 hydrotalcites with aqueous solutions of ammonium heptamolybdate at pH = 4.5 and 80 °C. These results confirm that, despite the low pH used, paramolybdate is unable to react with these cations giving rise to other solids.

Development of the grafting process upon heating at 80 °C has been also checked by rehydrating the solid after calcination at 120 °C; the corresponding PXRD diagram has been included in Figure 3; it should be remembered that calcinations between 80 and 200 °C give rise to solids whose PXRD diagrams only show the diffraction lines at 11−9.8 Å (2θ = 8.05−9.0°) and 4.9 Å. For these experiments, the solids calcined at 120 °C were stored for 1 day in a vacuum desiccator at saturation vapor pressure (water had been decarbonated previously). The diagrams for the MgAl−POM hydrotalcite rehydrated showed diffraction lines at 12−9.8, 6, and 4 Å, Figure 3A, similar to those in the original samples (not calcined). The intensity of the line at 4.9 Å (2θ = 18°) decreases upon rehydration being almost unobservable. So, we can safely conclude that this line (and probably another obscured by the broad diffraction between 11 and 9.8 Å) corresponds to another hydrotalcite phase (we will call it phase II), which is reversibly formed from the first phase (phase I, characterized by maxima at 12, 6, and 4 Å, corresponding to 2θ = 7.3, 14.7, and 22.2°, respectively). Despite the cautions taken during rehydration, a small portion of carbonate is intercalated, thus accounting for the diffrac-

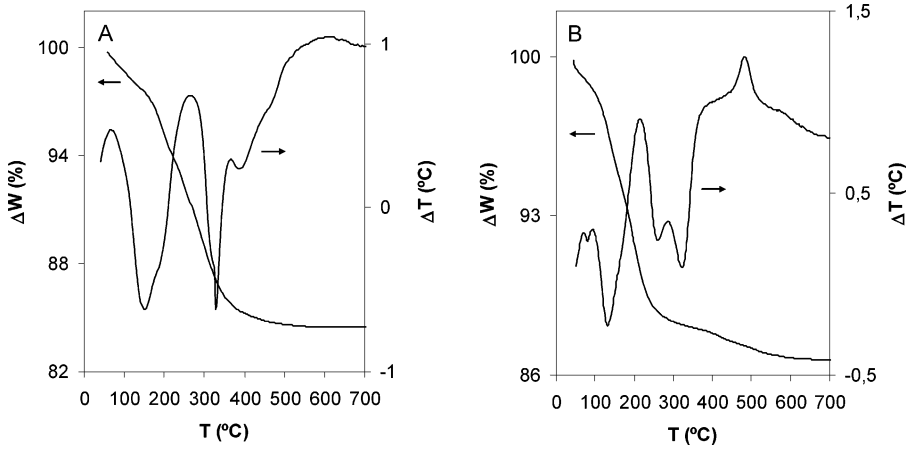

Figure 4. DTA/TG profiles recorded in N_2 atmosphere of samples (A) MgNMo and (B) ZnNMo.

tion line at 7.6 Å ($2\theta = 11.6°$), corresponding to (003) planes of the Mg,Al−CO_3 solid.[1,2] Only when the Zn-containing sample had been previously calcined between 80 and 100 °C, reversible rehydration occurred, Figure 3B. A small amount (lower than in the case of the Mg,Al sample) of carbonate is intercalated during rehydration, probably due to the lower basicity of the Zn-containing solids.

These results indicate that grafting does not take place and also that the phase existing in the calcined solids is not a poorly crystallized salt of the M^{2+}/M^{3+} cations, as in such a case the LDH-heptamolybdate structure would not have been recovered. Moreover, in the case of the Zn-containing samples the interaction between heptamolybdate and the brucite-like layers is stronger than in the case of the Mg-containing samples, and the interaction becomes more intense as the temperature is increased. These results are in agreement with the high-temperature transformations observed, as $ZnMoO_4$ is formed at a lower temperature (450−500 °C) than $MgMoO_4$ (600 °C).

Thermal Analysis (TG/DTG). The TG and DTG curves recorded for the heptamolybdate-containing LDHs are very similar, and so only the curves for one sample within each series are shown in Figure 4.

In both cases, weight is lost in a continuous step from ca. 100 to 400 °C. This weight loss is, however, due to several consecutive overlapped steps, as described by the DTA curves, also shown in the same figure.

The Mg-containing samples show two endothermic effects at 150 and 329 °C, which can be ascribed[2,3] to removal of water molecules adsorbed on the external surface of the crystallites, removal of interlayer water molecules (unfortunately, evolved gases could not be analyzed), and dehydroxylation of the layers, leading to collapsing of the layered structure. The weight loss associated to these processes is ca. 17% of the initial sample weight. A progressive weight loss is recorded for sample Zn,Al-heptamolybdate, Figure 4B, up to 500 °C, amounting ca. 15% of the initial sample weight, and corresponding to four endothermic peaks at 85, 136, 268, and 328; as for the Mg-containing samples, the first two peaks can be due to dehydration, and the next two peaks, to dehydroxylation. An additional exothermic peak at 480 °C can be tentatively ascribed to crystallization of $ZnMoO_4$, which presence has been confirmed by other techniques even for the sample calcined at 450 °C.

The results from the TG/DTA study are in agreement with the PXRD study for the samples calcined at increasing temperatures; calcination at 300 °C leads to amorphous solids, as collapsing and destruction of the layered structure starts at ca. 200−250 °C.

Raman Spectroscopy. When using exciting lines at 1064, 785, and 514 nm, the Raman spectra of the uncalcined Mo-containing LDHs show the same characteristics, implying the lack of resonance Raman effect at the laser wavelengths used. The spectra for samples MgNMo and ZnNMo, recorded with the 785 nm exciting line, are included in Figure 5; the spectra for the other samples were similar. The baseline of the spectra for samples calcined at 300 and 400 °C has been corrected because of the marked fluorescence background when excited at 514 nm, which considerably decreases at 785 nm and disappears at 1064 nm.

Assignment of the bands recorded is summarized in Table 2; some of them have been identified by deconvolution of the experimental spectra in the 270−420 and 720−1020 cm^{-1} ranges; the spectra are included in Figure 5.

The Raman spectra of molybdenum−oxygen isopolyanions exhibit[40−44] five characteristic ranges of vibrational modes at 200, 310−370, 500−650, 700−850, and 900−1000 cm^{-1}, which are usually assigned respectively to Mo−O−Mo deformations, Mo═O bending vibrations, symmetric Mo−O−Mo stretching, antisymmetric Mo−O−Mo stretching, and symmetric and antisymmetric terminal Mo═O stretching. All Zn,Al and Mg,Al samples show similar Raman spectra, with bands basically coincident with those of the heptamolybdate anion; the intense band recorded close to 200 cm^{-1} and the band at 550 cm^{-1} (ν_s(Mo−O−Mo)) are characteristic of highly polymerized species, although the band at 550 cm^{-1} can be also ascribed (together with another band at 470 or 490 cm^{-1}) to Al/Mg−OH or Zn/

(40) Aveston, J.; Anacker, E. W.; Johnson, J. S. *Inorg. Chem.* **1969**, *8*, 6.
(41) Kepert, D. L. *Comp. Inorg. Chem.* **1973**, *4*, 607.
(42) Griffith, W. P.; Lesniak, P. J. B. *J. Chem. Soc. A* **1969**, 1066.
(43) Zezlorowski, H.; Knözinger, H. *J. Phys. Chem.* **1979**, *83*, 1166.
(44) Hardcastle, F. D.; Wachs, I. E. *J. Raman Spectrosc.* **1990**, *21*, 683.

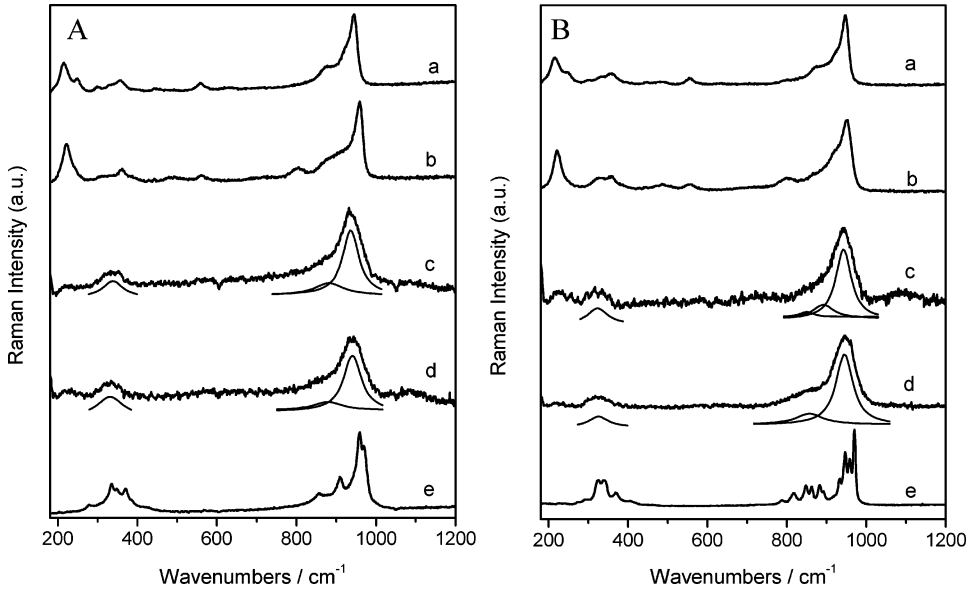

Figure 5. Raman spectra of the samples (A) MgNMo and (B) ZnNMo, excited with λ of 785 nm. Key: (a) originals samples and calcined at (b) 150, (c) 300, (d) 400, and (e) 700 °C.

Table 2. Assignment of the Bands (cm^{-1}) Recorded in the Raman Spectra of the Samples

sample	$\nu(Mo{=}O_t)_s$	$\nu(Mo{=}O)_{as}$	bending (Mo═O)	δ(Mo−O−Mo)
MgNMo	945	879	331, 357	216, 246
MgNMo/150	960	879, 803	334, 358	222
MgNMo/300	936	880	338	220 (vw)
MgNMo/400	941	880	332	220 (vw)
ZnNMo	946	880	330, 358	215, 245
ZnNMo/150	951	881, 803	326, 358	221
ZnNMo/300	942	890	323	226 (vw)
ZnNMo/400	945	856	326	226 (vw)
$Mo_7O_{24}^{6-}$	943	903	362	219
MoO_4^{2-}	897	837	317	

Al−OH translation modes of the brucite-like layers.[45] The small differences observed in the positions of the bands, from those for the free heptamolybdate anions, can be due to the interactions between the anion and the brucite-like layers.

The spectra for the samples calcined at 150 °C are very similar to those for the uncalcined samples, both due to polymolybdate species and to the hydrotalcite-like structure; the only difference is a slight shift toward larger wavenumbers of the band due to mode $\nu(Mo{-}O)_t$, especially for the Mg-containing sample (from 945 to 960 cm^{-1}). This shift has been ascribed by other authors to a decrease in the Mo−O bond length; Hardcastle and Wachs[44] have proposed the equation $R(Mo{-}O) = 0.48239 \ln(32895/\nu)$ to determine the Mo−O bond length from the position of this band. When applied to our results, it indicates that the heptamolybdate species existing in the original samples undergo a slight shortening of the Mo−O bonds upon calcination at 80−200 °C, probably as a consequence of a stronger interaction between the ispolyoxometalate unit and the brucite-like species.

The band at 330 cm^{-1}, recorded for the original and 150 °C calcined samples, corresponds to the δ(Mo═O) mode, but it can be due to an overlapping of the bands due to δ(Mo═O) of tetrahedral [MoO_4] (317 cm^{-1}) and octahedral [MoO_6] species (360 cm^{-1}), thus accounting for the presence of MoO_4^{2-} species together with heptamolybdate ones. However, their concentration should be very low, as from chemical analyses results for the original samples, a coherent chemical formula is calculated by assuming that all molybdenum is as heptamolybdate.

Upon calcination of the samples above 200 °C, Figure 5, despite that bands characteristic of octahedral [MoO_6] species are still recorded, the band at 200 cm^{-1}, due to mode δ(Mo−O−Mo), is weaker, indicating a lower polymerization degree; in addition, the δ(Mo═O) band is recorded between 325 and 340 cm^{-1}. Consequently, it seems that calcination at 300−400 °C, in addition to destroying the layered structure (the bands due to Al/Mg−OH and Zn/Al−OH translation modes are not longer recorded), also decreases the polymerization degree, increasing the concentration of tetrahedral [MoO_4] species, even probably forming dimolybdate species, containing tetrahedral and octahedral species.[44]

Upon calcination at 500 °C (samples Zn,Al-heptamolybdate), 600 °C (samples Mg,Al-heptamolybdate), or above, important changes are observed in the spectra. Those for the samples calcined at 700 °C are shown in Figure 5. The characteristic band of polymolybdates at 200 cm^{-1} is no longer recorded, but intense bands at 966, 955, 908, 852, 286, 330, and 365 cm^{-1} are recorded for the Mg,Al−heptamolybdate system. These bands are characteristic of crystalline monoclinic $MgMoO_4$[46] (which presence had been already detected by PXRD) where Mo^{VI} is octahedrally coordinated. For the Zn,Al−heptamolybdate sample, Figure 5B, the bands are recorded between 960 and 930 and 400−330 cm^{-1} and would correspond to Zn molybdate and dimolybdate, where Mo^{VI} ions are tetrahedrally and octahedrally coordinated, in agreement too with the PXRD data.

(45) Kloprogge, J. T.; Hickey, L.; Frost, R. L. *J. Raman Spectrosc.* **2004**, *35*, 967.

(46) Cadus, L. E.; Gómez, M. F.; Abello, M. C. *Catal. Lett.* **1997**, *43*, 229.

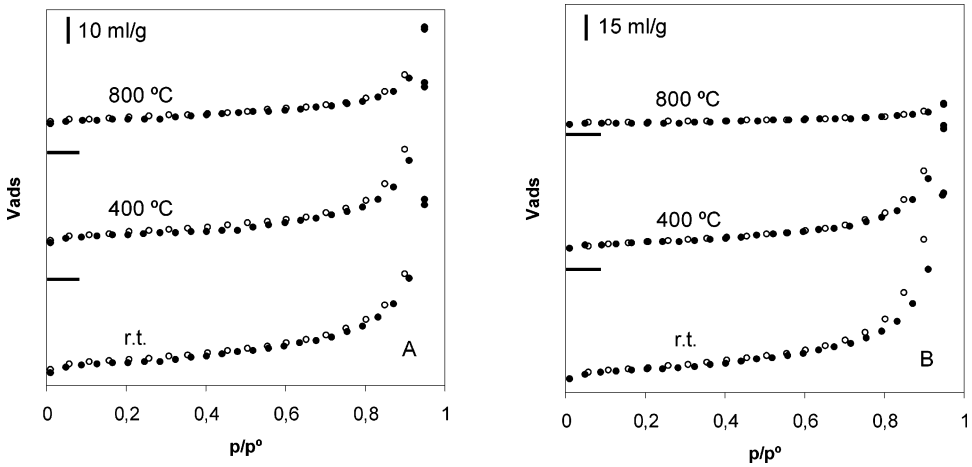

Figure 6. N_2 adsorption−desorptions isotherms for samples (A) MgTMo and (B) ZnTMo, calcined at the temperatures shown.

These results show that the interlayer molybdate species existing in all the original, uncalcined, samples are mainly heptamolybdate, coexisting with a small amount of tetrahedral [MoO_4] species; these tetrahedral species, formed via hydrolysis of heptamolybdate, would account for the broad PXRD effect recorded between 11 and 9.8 Å ($2\theta = 8.05-9.0°$). The layered structure and the same Mo-containing species seem to exist upon calcination at 80−200 °C, although in such a case the original and calcined samples would display the same gallery height (from their PXRD diagrams), unless the orientation of the interlayer anion would be different in phase II. However, this is not possible, as all orientations different from that for phase I (heptamolybdate units with its C_2 axis perpendicular to the layers) would give rise to larger gallery heights. Consequently, from the Raman spectra (shift of the $\nu(Mo{=}O)_t$ band to larger wavenumbers) we should conclude that heptamolybdate units in phase II should be slightly distorted, because of its interaction with the layers. This distortion is responsible for the diffraction line at 4.9 Å ($2\theta = 18.0°$) and probably another close to 10 Å ($2\theta = 8.8°$) obscured in the broad band recorded at 11−9.8 Å ($2\theta = 8.05-9.0°$) in the PXRD diagrams. The layered structure is destroyed when the samples are calcined at 300 °C (the characteristic Raman bands of LDHs are absent) and depolymerization starts; both tetrahedral and octahedral species coexist in these mostly amorphous phases, probably as dimolybdate units, which undergo further transformation when the calcination temperature is further increased, to crystalline Mg or Zn molybdates.

The increased concentration of tetrahedral species via depolymerization when the samples are calcined above the temperature required for destroying the layered structure is probably related to the increase in surface basicity of hydrotalcites upon dehydration and dehydroxylation, leading to formation of amorphous solids.

Specific Surface Area and Porosity. The nitrogen adsorption−desorption isotherms at −196 °C on some of the samples studied (both original and calcined ones) are included in Figure 6A and are characteristic of type I isotherms, although the weak inflection recorded would include them in type II of the IUPAC classification.[47] This sort of isotherm is typical of nonporous or microporous (pore diameter smaller than 2 nm) solids.

Table 3. Specific Surface Area ($m^2\ g^{-1}$) of the Samples Prepared

sample	S_{BET}	S_t	S_m	sample	S_{BET}	S_t	S_m
MgAlC	86						
MgAlN	26			ZnAlN	28		
MgAlT	1			ZnAlT	1		
MgMxMo	34						
MgNMo	31			ZnNMo	31		
MgTMo	30	17	13	ZnTMo	43	34	9
MgTMo/400	31	14	13	ZnTMo/400	32	23	8
MgTMo/800	20	10	10	ZnTMo/800	8	8	0

The values for the BET specific surface areas are summarized in Table 3. All Mg,Al−heptamolybdate samples show values close to 35 $m^2\ g^{-1}$, this value decreasing when the samples are calcined above 600 °C, probably because of the formation of crystalline $MgMoO_4$.

The largest specific surface area was measured for sample ZnTMo (43 $m^2\ g^{-1}$), while the terephthalate-containing precursors (MgAlT and ZnAlT) display the lowest values (1 $m^2\ g^{-1}$). For the Zn-containing samples, calcination at 500 °C decreases the specific surface area by 20%, due to crystallization of zinc molybdates, this effect being even more marked when the calcination temperature is increased up to 800 °C. The decrease in the specific surface area within the Zn series takes place at lower temperatures than for the Mg series, as for these samples crystallization of magnesium molybdates takes place at a higher temperature.

The t-curves[48] showing positive zero intercepts were confirming the presence of micropores. These plots were used to determine the external surfaces areas (from the slopes of the lines) and the area equivalent to adsorption in micropores (from the zero intercepts); the values have been summarized in Table 3. It should be noted that hydrotalcite-like materials with small interlayer anions (e. g., carbonate, nitrate, chloride, hydroxyl, etc.) are not microporous,[49] as the nitrogen molecules cannot access to the interlayer. In the samples here

(47) Sing, K. S. W.; Everett, D. H.; Haul, R. A. W.; Moscou, L.; Pierotti, R.; Rouquerol, J.; Sieminiewska, T. *Pure Appl. Chem.* **1985**, *57*, 603.
(48) Lippens, B. C.; de Boer, J. H. *J. Catal.* **1965**, *4*, 319.
(49) Rives, V. In *Layered Double Hydroxides: Present and Future*; Rives, V., Ed.; Nova Sci. Pub., Inc.: New York, 2001; Chapter 8, p 229.

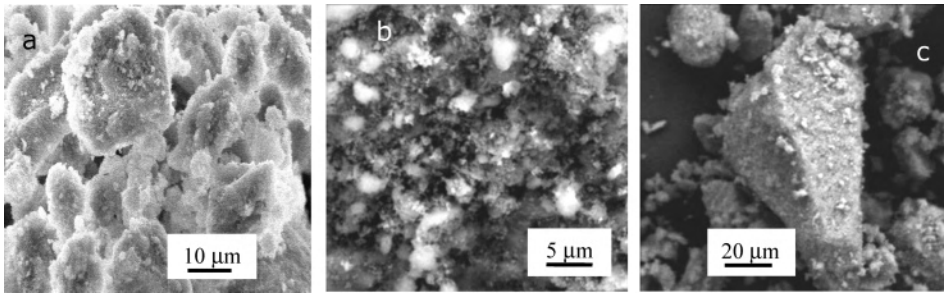

Figure 7. SEM micrographs of sample MgNMo (a) original and calcined at (b) 400 and (c) 800 °C.

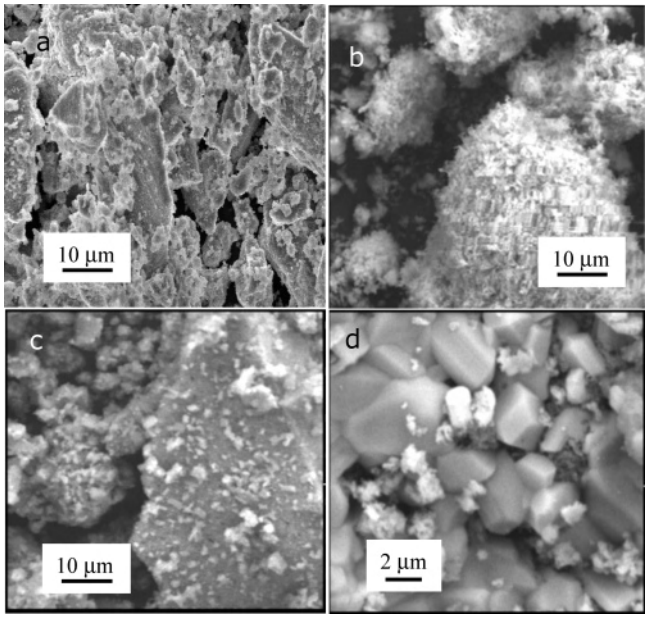

Figure 8. SEM micrographs of sample ZnNMo (a) original and calcined at (b) 400, (c) 800, and (d) 900 °C.

studied, however, the microporosity observed can be related to the incorporation of rather large anions, which have a swelling effect on the brucite-like layers, thus allowing insertion of nitrogen molecules in the interlayer space. Microporosity, however, decreases when the samples are calcined at increasing temperatures. Pore size distribution curves indicate that the main pores have a diameter between 1 and 2 nm in the original samples, while for those calcined at 800 °C the dominant pores have a diameter between 3 and 5 nm, probably being interparticle pores.

Electron Microscopy. The scanning electron micrographs for original and some calcined MgAl− and ZnAl−heptamolybdate samples are shown in Figures 7 and 8. The morphologies observed are rather similar. So, the original samples and those calcined up to 200 °C appear as agglomerates of layered particles with a diameter between 5 and 10 μm. The average size decreases to 2 μm when the samples are calcined between 200 and 700 °C. The apparent particle size does not change further when the calcination temperature is increased for the Mg,Al samples; however, calcination at 900 °C of the Zn-containing samples leads to formation of particles with a shape rather different from the others and which can be tentatively ascribed to formation of MoO_3 crystallites.

Conclusions

Although the use of LDH precursors with different anions in the interlayer, such as nitrate, hydroxide, and terephthalate, allows the intercalation of isopolyoxomolybdates, a faster anion exchange has been observed when using LDH-terephthalate as the starting material.

It can be concluded from the Raman spectra that molybdenum is present, mainly as heptamolybdate with some isolated molybdate species, in Zn and Mg systems, both uncalcined and calcined up to 250 °C. The differences observed in the PXRD patterns between the uncalcined samples and those calcined up to 250 °C are due to distortion of the octahedra, more evident when the calcination temperature is increased, as a consequence of a strong interaction between isopolyanions and the brucite-like layers. By a rehydration treatment, calcined samples recover their original Mo−O distances. When the samples are calcined between 300 and 400 °C, amorphous phases are obtained, in which the polymerization degree of the Mo-containing species is lower than in the uncalcined ones, they existing probably as dimolybdate, as both octahedral and tetrahedral oxo−molybdenum units are detected. Zn and Mg molybdates are formed at 450 and 600 °C, respectively. Calcination of zinc-containing samples above 600 °C gives rise to new crystalline phases identified as zinc dimolybdate and Zn−Al spinel, and finally, at 900 °C MoO_3 (detected by SEM) is formed.

Type I/II nitrogen adsorption isotherms, showing interlayer microporosity produced by the polyanion intercalation, are measured for all the solids prepared. The specific surface areas are not very large and decrease when the calcination temperature is increased, as a consequence of the formation of crystalline phases.

Acknowledgment. Financial support from the MEC (Grant MAT2003-06605-C02-01) and ERDF is acknowledged; D.C. acknowledges a grant from the Universidad de Salamanca.

IC0508674